Global Biogeochemical Cycles

RESEARCH ARTICLE
10.1029/2021GB006938

Drivers of Organic Molecular Signatures in the Amazon River

Martin R. Kurek[1], Aron Stubbins[2], Travis W. Drake[3], Jose M. S. Moura[4], R. Max Holmes[5], Helena Osterholz[6,7], Thorsten Dittmar[7,8], Bernhard Peucker-Ehrenbrink[9], Miyuki Mitsuya[4], and Robert G. M. Spencer[1]

[1]Department of Earth, Ocean and Atmospheric Science, Florida State University, Tallahassee, FL, USA, [2]Departments of Marine and Environmental Science, Department of Civil and Environmental Engineering, Department of Chemistry and Chemical Biology, Northeastern University, Boston, MA, USA, [3]Department of Environmental Systems Science, Swiss Federal Institute of Technology, ETH Zurich, Zurich, Switzerland, [4]Center for Interdisciplinary Formation, Federal University of Western Para, Santarém, PA, Brazil, [5]Woods Hole Research Center, Falmouth, MA, USA, [6]Marine Chemistry, Leibniz Institute for Baltic Sea Research Warnemünde, Rostock, Germany, [7]Institute for Chemistry and Biology of the Marine Environment (ICBM), University of Oldenburg, Oldenburg, Germany, [8]Helmholtz Institute for Functional Marine Biodiversity (HIFMB) at the University of Oldenburg, Oldenburg, Germany, [9]Woods Hole Oceanographic Institution, Woods Hole, MA, USA

Abstract As climate-driven El Niño Southern Oscillation (ENSO) events are projected to increase in frequency and severity, much attention has focused on impacts regarding ecosystem productivity and carbon balance in Amazonian rainforests, with comparatively little attention given to carbon dynamics in fluvial ecosystems. In this study, we compared the wet 2012 La Niña period to the following normal hydrologic period in the Amazon River. Elevated water flux during the La Niña period was accompanied by dilution of inorganic ion concentrations. Furthermore, the La Niña period exported 2.77 Tg C yr^{-1} more dissolved organic carbon (DOC) than the normal period, an increase greater than the annual amount of DOC exported by the Mississippi River. Using ultra-high-resolution mass spectrometry, we detected both intra- and interannual differences in dissolved organic matter (DOM) composition, revealing that DOM exported during the dry season and the normal period was more aliphatic, whereas compounds in the wet season and following the La Niña event were more aromatic, with ramifications for its environmental role. Furthermore, as this study has the highest temporal resolution DOM compositional data for the Amazon River to-date we showed that compounds were highly correlated to a 6-month lag in Pacific temperature and pressure anomalies, suggesting that ENSO events could impact DOM composition exported to the Atlantic Ocean. Therefore, as ENSO events increase in frequency and severity into the future it seems likely that there will be downstream consequences for the fate of Amazon Basin-derived DOM concurrent with lag periods as described here.

Plain Language Summary Increases in atmospheric carbon concentrations originate from many sources and pose a serious threat to global ecosystem health and humanity. The Amazon River delivers one-fifth of global discharge and represents the largest single flux of dissolved organic carbon (DOC) from land to ocean. As climate change is projected to increase precipitation anomalies throughout the Amazon, flooding and droughts will become more frequent and severe, disrupting the natural seasonal rhythm of the Amazon River. We demonstrate that precipitation anomalies in South America (caused by La Niña) exported an additional amount of DOC from the Amazon River to the Atlantic Ocean than the Mississippi River exports annually. Organic compounds mobilized during the La Niña were more aromatic, presumably from terrestrial sources. These compositions, measured near the mouth of the Amazon River, arrived six months after Pacific sea-surface temperature and pressure anomalies indicated the onset of La Niña, highlighting the lag time that events in the Pacific take to impact the Atlantic Ocean.

Key Points:

- The Amazon River during a La Niña year exports an additional amount of dissolved organic carbon than the Mississippi exports annually
- The Amazon River dissolved organic matter composition in a La Niña year was more oxidized and aromatic than during a non-ENSO year
- The dissolved organic matter composition in the Amazon River correlates to a 6-month lag with La Niña indices

Supporting Information:

Supporting Information may be found in the online version of this article.

Correspondence to:

M. R. Kurek,
mrk19f@my.fsu.edu

Citation:

Kurek, M. R., Stubbins, A., Drake, T. W., Moura, J. M. S., Holmes, R. M., Osterholz, H., et al. (2021). Drivers of organic molecular signatures in the Amazon River. *Global Biogeochemical Cycles*, *35*, e2021GB006938. https://doi.org/10.1029/2021GB006938

Received 6 JAN 2021
Accepted 28 MAY 2021

Author Contributions:

Conceptualization: Aron Stubbins, Jose M. S. Moura, R. Max Holmes, Bernhard Peucker-Ehrenbrink, Robert G. M. Spencer
Data curation: Martin R. Kurek, Robert G. M. Spencer
Formal analysis: Martin R. Kurek
Funding acquisition: R. Max Holmes, Bernhard Peucker-Ehrenbrink, Robert G. M. Spencer
Investigation: Aron Stubbins, Jose M. S. Moura, R. Max Holmes, Miyuki Mitsuya, Robert G. M. Spencer
Methodology: Aron Stubbins, Travis W. Drake, Jose M. S. Moura, Helena Osterholz, Thorsten Dittmar, Bernhard Peucker-Ehrenbrink, Miyuki Mitsuya, Robert G. M. Spencer
Project Administration: Aron Stubbins, Jose M. S. Moura, R. Max

1. Introduction

Inland waters have been increasingly recognized as hotspots for global carbon cycling, moving away from being viewed as passive transporters and reservoirs, to being accepted as interwoven conveyers and reactors (Battin et al., 2009; Cole et al., 2007; Drake et al., 2018; Tranvik et al., 2009). Dissolved organic matter

Holmes, Bernhard Peucker-Ehrenbrink, Robert G. M. Spencer
Resources: Aron Stubbins, Travis W. Drake, Jose M. S. Moura, Helena Osterholz, Thorsten Dittmar, Bernhard Peucker-Ehrenbrink, Miyuki Mitsuya, Robert G. M. Spencer
Software: Martin R. Kurek, Aron Stubbins, Travis W. Drake, Thorsten Dittmar
Supervision: Aron Stubbins, Robert G. M. Spencer
Validation: Aron Stubbins, Travis W. Drake, Robert G. M. Spencer
Visualization: Martin R. Kurek
Writing – original draft: Martin R. Kurek
Writing – review & editing: Martin R. Kurek, Aron Stubbins, Travis W. Drake, Jose M. S. Moura, R. Max Holmes, Helena Osterholz, Thorsten Dittmar, Bernhard Peucker-Ehrenbrink, Robert G. M. Spencer

(DOM) is a major component of freshwater carbon dynamics and represents a complex mixture of molecules from various terrestrial and aquatic sources with many ecosystem functions, ultimately serving as one of the most important intermediaries in the global carbon cycle (Battin et al., 2009). The reactivity or persistence of DOM is related to both the local environmental conditions and its intrinsic chemical composition (Amon & Benner, 1996a; Amon & Benner, 1996b; Aufdenkampe et al., 2001; Kellerman et al., 2018; Spencer et al., 2013). Ultra-high-resolution Fourier transform-ion cyclotron resonance mass spectrometry (FT-ICR MS) has been adopted in recent years as the most comprehensive technique for characterizing DOM composition as well as linking this to lability, revealing potential sources and degradation processes within heterogenous mixtures (Gonsior et al., 2016; Kellerman et al., 2018; Kurek et al., 2020; Lechtenfeld et al., 2014; Riedel et al., 2016; Stubbins et al., 2010). Many of these compositional differences are driven by in situ processing during riverine transport (Amon & Bener, 1996a; Stubbins et al., 2010; Vannote et al., 1980), which is responsible for both producing new compounds, mineralizing DOM to CO_2, and linking terrestrial carbon to the atmospheric and marine reservoirs (Aufdenkampe et al., 2011; Battin et al., 2009; Drake et al., 2018; Hedges et al., 1997). Riverine export of DOC is approximately 250 Tg C annually and provides the largest flux of reduced carbon from terrestrial to marine environments (Hedges et al., 1997), with the Amazon River responsible for over 10% of the land-ocean DOC flux alone (Moreira-Turcq et al, 2003; Raymond & Spencer, 2015; Richey et al., 1990).

The Amazon is the largest river on Earth by discharge and drainage area, contributing almost 20% of the global riverine discharge to the ocean and draining a massive basin of over 6×10^6 km^2 (Raymond & Spencer, 2015). The Amazon River transports inorganic solutes, which are diluted with increasing discharge, and biogenic solutes, which are enriched with discharge; the so-called "rhythm" of the Amazon (Devol et al., 1995; Drake et al., 2021; Moquet et al., 2016; Richey et al., 1990). Among the biogenic solutes, DOM is transported from the high Andes, grasslands, forests, and floodplains, and continually processed on the journey to the Atlantic Ocean (Aufdenkampe et al., 2007; Benner et al., 1995; Seidel et al., 2016; Ward et al., 2013). Though the fate of the DOM varies, the majority is thought to be directly exported into the Amazon River coastal plume downstream (Medeiros et al., 2015; Seidel et al., 2015), whereas the more photo- and biolabile compounds are thought to be mineralized instream (Amon & Benner, 1996b; Quay et al., 1992; Ward et al., 2013). Given that the Amazon River outgasses an estimated 0.47–1.4 Pg C $year^{-1}$ as CO_2 to the atmosphere (Richey et al., 2002; Sawakuchi et al., 2017), the high DOC concentrations of its tributaries (Moreira-Turcq et al, 2003), and the microbial preference to respire biolabile DOM (D'Andrilli et al., 2019; Valle et al., 2018), it is likely that a portion of Amazon riverine DOM contributes to atmospheric CO_2 fluxes (Mayorga et al., 2005; Ward et al., 2013).

Changes in climate and land use are expected to alter the feedback between atmospheric and aquatic carbon export from the Amazon Basin (Aufdenkampe et al., 2011; Spencer et al., 2019). Periodic anomalies in Pacific sea surface temperatures and air pressures result in events known as the El Niño Southern Oscillation (ENSO), where periods of warmer Pacific sea surface temperatures are termed El Niño years, and periods of colder Pacific sea surface temperatures are called La Niña years. Historical trends suggest that La Niña events contribute to increased precipitation anomalies leading to colder and wetter conditions in the Amazon Basin, while El Niño events cause decreased precipitation anomalies leading to warmer and drier conditions (Foley et al., 2002; Ronchail et al., 2005). These variations in precipitation have resulted in regional flooding during La Niña years and droughts in El Niño years across the Amazon Basin (Espinoza et al., 2013; Marengo et al., 2013), both of which influence the annual discharge of the mainstem and its downstream catchments (Foley et al., 2002; Richey et al., 1989; Ronchail et al., 2005). Anthropogenic climate change has amplified the effects of ENSO cycles on the Amazon Basin, with both El Niño and La Niña events expected to increase in severity and frequency (Cai et al., 2015; Widlansky et al., 2015). Long term studies have also found that over the past 30 years, the Amazon River has experienced an amplification of seasonality where the maximum discharge has increased during wet seasons and the minimum discharge has decreased during dry seasons (Liang et al., 2020). These swings in seasonal discharge from the Amazon River have had additional long-term effects on downstream geochemical properties including salinity within the Amazon Plume as well as potentially affecting marine biogeochemistry and global carbon cycling (Liang et al., 2020).

While multi-year Amazon River DOC fluxes have been assessed (Moreira-Turcq et al, 2003; Richey et al., 1990), DOM compositions have been restricted to discrete sampling campaigns encompassing limited seasonal coverage with large gaps between annual wet and dry seasons (Gonsior et al., 2016; Medeiros et al., 2015; Seidel et al., 2015; Seidel et al., 2016). For example, Medeiros et al. (2015) collected DOM samples during three periods between 2010 and 2012 (two at high discharge and one a low discharge). Seidel et al. (2015) collected samples during one period in July 2012 (high discharge), and both Ward et al. (2015) and Seidel et al. (2016) examined five sampling periods from the Amazon River between 2010 and 2012 (two at low discharge, one on the rising limb of the hydrograph, one at peak discharge, and one on the falling limb). Several of these studies have suggested that the composition of terrestrial DOM exported from the Amazon River to the Atlantic Ocean varies with seasonal hydrology, while earlier work has hypothesized that mainstem organic matter components are invariant with respect to discharge due to processing during transport (Ertel et al., 1986; Hedges et al., 1986; Hedges et al., 1994). Ultimately, these previous studies of Amazon River DOM are limited with respect to their temporal resolution in being able to compare compositional changes between seasons. Even the most detailed temporal study only encompassed five samples over two years and was unable to account for the effects of ENSO on riverine DOM compositions and geochemical properties between years, nor were they able to assess the lag time between the onset of ENSO and when the changes in geochemical properties would occur (Seidel et al., 2016). In this study, we investigate DOC concentrations, geochemical indices, and DOM compositions from the Amazon River spanning an ENSO event at a near monthly sampling frequency for over two years, thus allowing us to directly assess the lag time between ENSO indices and riverine geochemistry. Specifically, we compare DOC fluxes and DOM properties between a La Niña and a consecutive non-ENSO (hydrologically normal) period.

2. Materials and Methods

2.1. Study Site and Sampling

Near-monthly water sampling from July 22, 2011 to November 16, 2013 (Table S1) was conducted in the Amazon mainstem at the furthest downstream Brazilian National Water Agency (https://www.ana.gov.br) gauging station (17050000) at Óbidos (1°56′S 55°30′W) (Figure 1), where over 90% of the DOC flux from the Amazon to the Atlantic Ocean is captured (Raymond & Spencer, 2015). During each sampling date, three water samples (1 L) were collected at 0.5 m depth from the river at the gauging station across the channel in equal spacing. The samples were combined into a 4 L carboy to make a composite sample and filtered through a 0.45 μm capsule filter using a peristaltic pump and tubing into polycarbonate bottles. The filtered samples were immediately frozen and kept in the dark until analysis. River discharge measurements were taken from the gauging station the same day as water samples.

Monthly values for the Southern Oscillation Index (SOI) were obtained from the Australian Government Bureau of Meteorology (2020) and values for the Oceanic Niño Index (ONI) were obtained from the National Oceanic and Atmospheric Administration (National Weather Service Climate Predicition Center Cold & Warm Episodes by Season, 2020) for the period of June 2010–November 2013.

2.2. Geochemical Analysis and Modeling

DOC was measured on filtered samples by high-temperature combustion using a Shimadzu TOC-V organic carbon analyzer and established methods (Mann et al., 2012). DOC concentrations were calculated from the mean of three injections having a coefficient of variance <2% and fit to a 6-point calibration curve. An internal standard was analyzed periodically to assess any baseline drift. The total precision between independent measurements was <5%.

Daily discharge and DOC fluxes were calculated using the FORTRAN Load Estimator (LOADEST) program (Runkel et al., 2004) and then summed to calculate annual loads for the La Niña year (August 2011–July 2012) and the following non-ENSO year (August 2012–July 2013). The calibration equation was derived using the Adjusted Maximum Likelihood Estimator (AMLE) and the regression model number was set to default (MODNO = 0), allowing for selection of the best model based on Akaike Information Criteria. The validity of the model was verified from the output of the R^2 of the AMLE, residuals data, and the serial

Figure 1. Amazon River Basin (highlighted area) with Óbidos sampling site (red point) and upstream drainage area (yellow outline).

correlation of residuals including confirmation that the residuals were normally distributed according to previous methods (Dornblaser & Striegl, 2009).

Anion concentrations (Cl^- and SO_4^{2-}) were measured using a Dionex ion chromatography system using a modified procedure outlined in Voss et al. (2014). Undiluted samples were injected twice onto an anion column (IonPacAS15, 4 mm, with ASRS 300 suppressor) and eluted with 50% 75 mM NaOH and 50% Milli-Q water. Analytical response was evaluated against serial dilutions using an internal standard (SpecPure ion chromatography standards; Alfa Aesar) and IAPSO standard seawater certified reference material (CRM, Batch P160). Final concentrations were calculated using a 5-point calibration curve with Chromeleon software and no blank correction. Certified reference material (CRM) concentrations were always within ±3% of reported values for Cl^- and SO_4^{2-}.

Cation concentrations (Na^+, Mg^{2+}, K^+, Ca^{2+}) were determined from single collect, inductively coupled plasma, magnetic sector mass spectrometry (ICPMS) using the Thermo Scientific Element2 ICMPS at the WHOI Plasma Facility with methods described in Voss et al. (2014) and Brown et al. (2020). Water samples (1.8 mL) were pipetted into 2 mL screwcap autosampler vials and centrifuged (10 min at 7,000 rpm) in a clean laboratory. The supernatant (1 mL) was transferred to another 2 mL vial and small amounts of indium and rhenium internal standards were added and the pH was adjusted to ≤2 with HNO_3. The concentrations of the internal standard isotopes were adjusted such that typical count rates were ~500,000 counts per second (cps, 10^{11} Ω resistor). Sample vials were placed on a vibrating shaker before being loaded into an autosampler and analyzed by self-aspiration at medium (m/Δm ~3,000, Ca) and high (m/Δm ~ 10,000, Na, Mg, K) mass resolving powers. Concentrations were determined with 7-point calibration curves using serial dilutions of NIST 1640a and SLRC-5 (National Research Council Canada) as CRMs. Whenever possible, count rates were collected for more than one isotope per element in order to check for the presence of isobaric interferences. Analytical blanks were prepared identical to the samples using Milli-Q water. Analytical results were corrected for blank, drift and isobaric interferences. External reproducibility (2 standard

deviation) was generally within ±5%. Samples were acidified and measured for SiO_2 using colorimetry on an Astoria Analyzer with methods modified from Mann et al. (2012).

2.3. Solid Phase Extraction

Filtered water samples were extracted for FT-ICR MS analysis with Varian Bond Elut PPL columns (25 mg) as described by Dittmar et al., 2008. Briefly, columns were rinsed with Milli-Q water acidified to pH 2 with concentrated HCl, conditioned with methanol, and rinsed once more with pH 2 Milli-Q water. Water samples (~20 mL) acidified to pH 2 were then passed through the columns via gravity. Columns were then rinsed with pH 2 Milli-Q water, dried under argon gas, and the DOM was eluted with high-purity methanol into precombusted glass vials. The vials were stored in the dark at −20°C prior to FT-ICR MS analysis.

2.4. Fourier Transform-Ion Cyclotron Resonance Mass Spectrometry (FT-ICR MS)

The DOM-methanol extracts were diluted using Milli-Q water and methanol to a final DOC concentration of 5 mg C L^{-1} and a methanol:water volume ratio of 1:1 then continuously infused into the electrospray ionization source of a Bruker Solarix 15 T FT-ICR MS instrument (University of Oldenburg, Germany). The flow rate was 120 μL hr^{-1} in negative mode and 200 scans were acquired for each sample. Instrument sensitivity was monitored using a standard reference material (NELHA extracted marine DOM). Raw mass spectra were calibrated using a reference mass list to a mass accuracy of less than 0.1 ppm. Only peaks above the method detection limit were considered (Riedel & Dittmar, 2014).

Mass lists were aligned according to m/z. Formulae containing $C_{2–60}$, $H_{2–122}$, $O_{1–34}$, $N_{0–4}$, $S_{0–2}$, and $P_{0–1}$ were then assigned to matched mass spectral peaks using in-house developed software according to previously published rules (Stubbins et al., 2010). The spectra were then blank corrected by removing contamination peaks found in PPL extracted methanol blanks. Chemical properties including the stoichiometric ratios of heteroatoms to carbon (e.g., H/C, O/C, N/C, etc.), modified aromaticity index (AI_{mod}) (Koch & Dittmar, 2006, 2016), and average carbon oxidation state (C_{OX}) (Mann et al., 2015) were calculated using abundance-weighted elemental counts from the assigned molecular formulae. The abundance-weighted average of formulae within the Island of Stability (IOS) was defined as formulae with $1.04 < H/C < 1.3$, $0.42 < O/C < 0.62$, $332 < m/z < 338$, and $446 < m/z < 548$ after Lechtenfeld et al. (2014) and the percent relative abundance of formulae contained in this group was computed for all samples.

2.5. Statistical Methods

Post processing and statistical analysis of the molecular formulae were conducted using Microsoft Excel and *R* with the ggplot2 package (Wickham, 2016). Differences in chemical compositions between years were evaluated by performing a two-sample T test at the $\alpha = 0.05$ significance level. The percent dissimilarity between all samples was calculated using a Jaccard matrix with the Jaccard index ranging from 0 to 100 where 0 is identical and 100 is completely dissimilar. Additionally, formulae common in all samples were pooled together and compared to each individual using the Jaccard index with their resulting dissimilarities fit to a loess regression through time.

Spearman correlations between the relative abundance of all Amazon River formulae, Oceanic Niño Index (ONI), and Southern Oscillation Index (SOI) values from a 0 to 12-month lag were calculated using the psych package in *R* (Revelle, 2017). Significantly correlated formulae between each lagged index were only considered if they had a false discovery rate corrected *p*-value ($p < 0.05$) (Benjamini & Hochberg, 1995).

3. Results and Discussion

3.1. Interannual Differences in Amazon River Hydrology

Sampling of the Amazon River began during mid (July) 2011 and was conducted through the end (November) of 2013 at a near-monthly frequency, allowing for the resolution of temporal trends in discharge, inorganic geochemistry, DOC, and DOM composition within two annual pulses of the hydrograph (Figure 2, pink shaded region; Table S1). The beginning of our sampling period coincided with the onset of the

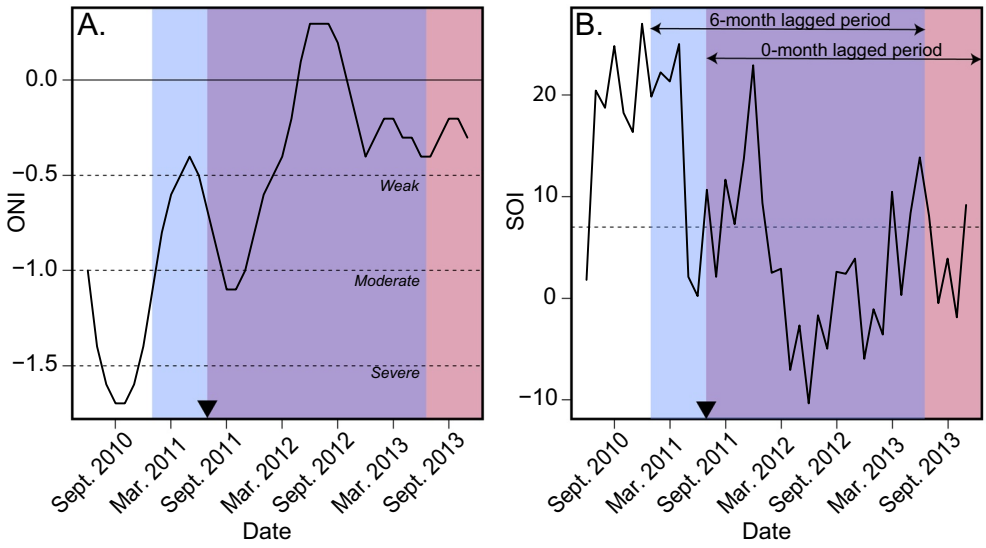

Figure 2. (a) Monthly Oceanic Niño Index (ONI) from June 2010 to November 2013 with data obtained from the National Oceanic and Atmospheric Administration (NOAA). Values below −1.5 indicate a strong La Niña event, values between −1.0 and −1.5 indicate a moderate La Niña event and values between −0.5 and −1.0 indicate a weak La Niña event. (b) Monthly Southern Oscillation Index (SOI) from June 2010 to November 2013 with data obtained from the Australian Government Bureau of Meteorology. Sustained SOI values above seven (dashed line) are typical of La Niña events. The black triangle denotes the start of the samples collected in this study. The shaded pink regions correspond to the months from the study period (July 2011–November 2013) and a 0-month lag in index values. The shaded blue region spans index values 6 months prior to the start of the study period illustrating a 6-month lag. The overlap between the regions signifies SOI and ONI values that occurred during both the 0-month and 6-month lag periods.

2011–2012 La Niña event, continued through 2013, and ended just before a period of anomalous and intense rainfall at the end of 2013 (Espinoza et al., 2014). La Niña events were characterized using the Oceanic Niño Index (ONI) which has been utilized by NOAA to identify the severity of ENSO events using temperature anomalies in the east-central Equatorial Pacific (Figure 2a). ONI values below −0.5 are indicative of a La Niña event, with more negative values indicating a greater severity (Figure 2a). The ONI in this study also closely followed the Southern Oscillation Index (SOI) (Figure 2b), which is used as an additional indicator for ENSO developments. SOI values are calculated using sea-level atmospheric pressure differences between Darwin, Australia and Tahiti, French Polynesia, with sustained values above seven suggestive of a La Niña (Figure 2b).

The La Niña event resulted in early and widespread precipitation across the Northern and Western Amazon Basin starting in late 2011 with record flooding occurring in the tributaries feeding into the Amazon mainstem, while other regions received normal or even less rainfall (Espinoza et al., 2013; Marengo et al., 2013). The impacts of the La Niña could be seen at the furthest downstream gauging station and our sampling site in Óbidos, Brazil (Figure 1), where peak discharge in mid-May 2012 (~270,000 $m^3 s^{-1}$) occurred nearly two weeks earlier than in the previous and following years (Figure 3). Following the wet season in 2012, precipitation and discharge patterns returned to normal (defined here as non-ENSO, $-0.5 < ONI < 0.5$) until the end of 2013 (Figure 3a). We denote the normal year strictly in terms of ENSO indices ($-0.5 < ONI < 0.5$) and recognize that characterizing a hydrologically "normal" year for the Amazon River would require long time series of discharge and flux calculations. However, our data still suggests that two distinct hydrological regimes spanned the course of the study in the Amazon River; the anomalous wet period influenced by the La Niña event (La Niña year) and the following period (normal year).

In the context of this study, we define the La Niña year from August 2011 to July 2012 (Figure 3, green shaded region) and the following normal year from August 2012 to July 2013 (Figure 3, blue shaded region). Although this period excludes several of our samples from 2011 and late 2013, this division allows for an even comparison between the years and was chosen for two reasons. First, the samples from mid 2011 to late 2013 were separated into two equivalent hydrologic years for each to capture an entire pulse of the Am-

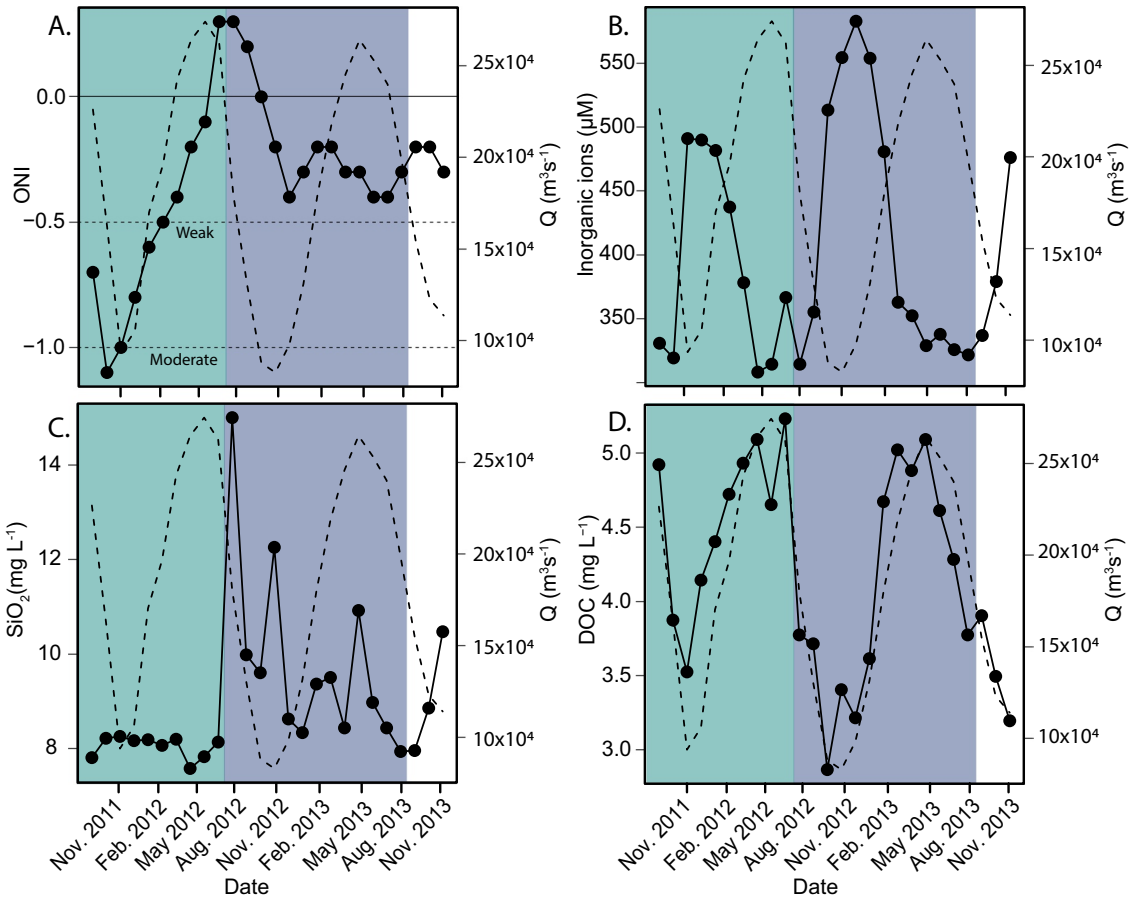

Figure 3. (a) Line plot of the Oceanic Niño Index during the study period with a weak La Niña event in the region of −0.5 to −1.0 and a moderate La Niña in the region of −1.0 to −1.5. Line plots of (b) major inorganic ions (Cl^-, SO_4^{2-}, Ca^{2+}, Mg^{2+}, Na^+, K^+), (c) SiO_2, and (d) dissolved organic carbon measured at Óbidos during the study period. Discharge (Q) is indicated by the dashed line and study periods are divided into the La Niña year (August 2011–July 2012; green) and the normal year (August 2012–July 2013; blue).

azon River hydrograph. Both years started on the falling limb, encompassed both the yearly minimum and maximum discharge, and ended on the falling limb of the following calendar year. Second, correlations between Amazon River discharge and ENSO indices are not instantaneous with the effects of ENSO detected in Óbidos after a 6-month lag from the ONI and SOI (Foley et al., 2002; Richey et al., 1989). In other words, ENSO indices measured in the Pacific 6 months prior to river water sampling in the Amazon at Óbidos predetermined the fate of the Amazon River water when it was sampled and shifted the window of the ONI and SOI values that one must consider back in time by 6 months (Figure 2, blue shaded region). By February 2012, ONI values had increased (>−0.5), signifying the end of a moderate La Niña period in the Pacific, but the effects on discharge at Óbidos would still occur for about 6 months, ending around July 2012. Therefore, the discharge period after July 2012 would no longer have been influenced by the La Niña event and was denoted as the start of the normal year.

3.2. ENSO-Driven Changes in Amazon River Flux and Solute Export

Although extensive multi-year time series of Amazon River discharge fluxes, and solutes are currently unavailable to establish long term trends, we present strong evidence that ENSO-driven events likely influence the discharge flux as well as solute concentrations and compositions of the Amazon River. During the La Niña year, the Amazon River had a total discharge flux of 5,849 $km^3\ yr^{-1}$ while the normal year discharge flux of the Amazon River was only 5,578 $km^3\ yr^{-1}$. When compared to historical annual discharge measurements from the Amazon River, the La Niña year discharge from this study was greater than the

mean annual discharge from 1980 to 2000 and outside the upper 99% confidence interval (5,346 km^3 yr^{-1}, 5,043–5,649 km^3 yr^{-1}, 99% CI) (Hastie et al., 2019). For context, the difference between the normal year discharge and La Niña year discharge (271 km^3 yr^{-1}) amounted to more water exported into the Atlantic Ocean from the Amazon River than the Yukon River delivers to the Arctic Ocean each year (203 km^3 yr^{-1}) (Spencer et al., 2013).

The distinction between the years was also supported using inorganic geochemical measurements from the Amazon mainstem at Óbidos. Major dissolved inorganic ions (Cl^-, SO_4^{2-}, Ca^{2+}, Mg^{2+}, Na^+, K^+) sourced primarily from the Andes (Moquet et al., 2016) displayed predictable seasonal variability with higher concentrations in the dry period and lower concentrations in the wet period due to dilution (Devol et al., 1995; Drake et al., 2021; Moquet et al., 2016) (Figure 3b). However, monthly concentrations during the low discharge period were attenuated during the La Niña year (Figure 3b, green shaded region) indicating greater dilution from the widespread precipitation that occurred in the Northern and Western sub-basins at that time (Espinoza et al., 2013). Average SiO_2 concentrations were also significantly higher during the normal year (9.94 ± 1.96 vs. 8.02 ± 0.23 mg L^{-1}, $p = 0.006$; Figure 3c) reflecting the greater proportion of Andean water passing through Óbidos during the La Niña and diluting locally weathered Si from lower Amazon reaches (Devol et al., 1995; Drake et al., 2021; Moquet et al., 2016).

While the inorganic solute concentrations are controlled by dilution, biogenic solute concentrations typically correlate positively with discharge in terrestrial riverine systems (Pang et al., 2021; Rose et al., 2018; Spencer et al., 2013). Indeed, DOC concentrations increased with discharge at Óbidos (Figure 3d), likely driven by greater overland flow and input of terrestrial DOM from surface litter and organic soil horizons (Pang et al., 2021; Rose et al., 2018; Spencer et al., 2016). Average DOC concentrations between the years did not differ significantly, which is typical of the stable DOC concentrations in the mainstem (Richey et al., 1990). However, the flux of DOC from the Amazon was ~10% higher in the La Niña year (26.86 Tg C) than in the normal year (24.09 Tg C) by 2.77 Tg C yr^{-1}, amounting to additional DOC export greater than from the Mississippi River each year (~2.10 Tg C yr^{-1}) (Spencer et al., 2013). Thus, while Amazon River DOC concentrations have previously only been shown to vary by ~5% during this time period (Seidel et al., 2016), our higher frequency temporal sampling suggests that periodic ENSO events could export more DOC from the Amazon to the Atlantic Ocean at a scale that is greater than, or comparable to, the total DOC export of a number of major world rivers (e.g., Mississippi, Ganges, Brahmaputra, Yukon, St. Lawrence, Changjiang) (Raymond and Spencer, 2015; Spencer et al., 2013).

3.3. Seasonal Trends in Amazonian DOM Composition

Across the study period, wet season DOM contained compounds that were of higher molecular weight (MW), more oxidized, and aromatic than in the dry season which were of lower MW, reduced, and more aliphatic (Figures 4a–4c). These compositional differences can be interpreted in the context of bioavailability for heterotrophs because smaller, reduced, and aliphatic compounds are typically more biolabile, whereas larger, aromatic, and oxygenated compounds are usually more stable on the timescales considered here (D'Andrilli et al., 2015; Riedel et al., 2016; Textor et al., 2019). These trends are consistent with previous Amazonian DOM compositions from Óbidos, where aromatic compounds were relatively enriched at peak discharge (Drake et al., 2021; Seidel et al., 2016), as well as from other high discharge (Mann et al., 2014; Pang et al., 2021; Spencer et al., 2016) and arctic (Johnston et al., 2018; Spencer et al., 2008; Stedmon et al., 2011) rivers, with their diverse compositions suggesting heterogeneous sources. Riverine aromatic and oxygenated compounds typically originate from organic soil horizons and fresh plant litterfall that are mobilized during periods of increased hydrological connectivity, whereas microbial DOM is leached from deeper subsurface soil and groundwater under baseflow (McLaughlin & Kaplan, 2013; Wagner et al., 2019). Consequently, DOM during seasonal high-discharge events is exported to the ocean with a greater relative contribution from the molecular "island of stability" (IOS) which is composed of unsaturated and moderately oxygenated CRAM-like compounds that are considered refractory and suggested to persist for tens of thousands of years in the ocean as part of marine DOM (Lechtenfeld et al., 2014) (Figure 4d). Although IOS compounds were more abundant during high discharge events (Figure 4d), they were still relatively minor compared to the IOS content of marine DOM, and DOM from a variety of global rivers (Kellerman et al., 2018; Lechtenfeld et al., 2014; Pang et al., 2021). Given that IOS content has been shown to be inversely proportional

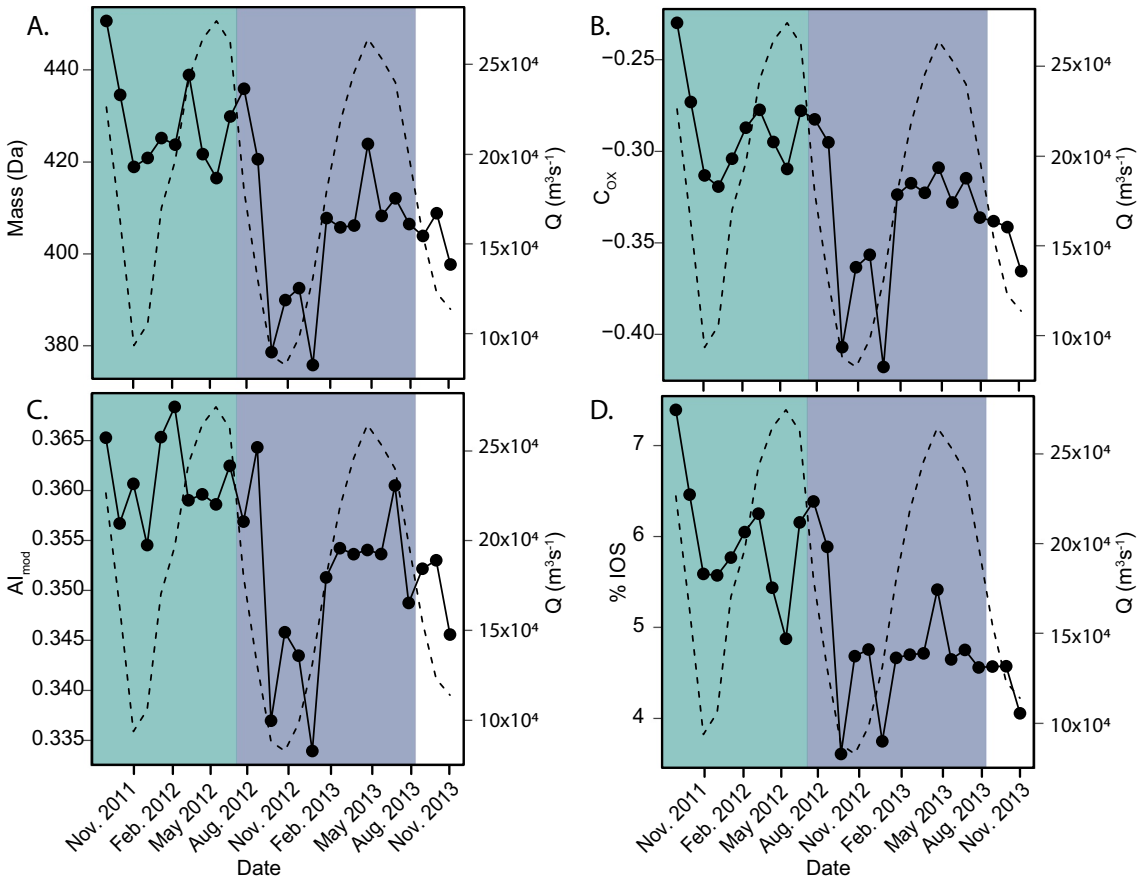

Figure 4. Line plots of dissolved organic matter properties from Óbidos during the study period including (a) average mass, (b) average carbon oxidation state (C_{OX}), (c), average modified aromaticity index (AI_{mod}), and (d) percent Island of Stability (IOS). Discharge (Q) is indicated by the dashed line and study periods are divided into the La Niña year (August 2011–July 2012; green) and the normal year (August 2012–July 2013; blue).

to $\Delta^{14}C$ across a diverse range of aquatic ecosystems (Kellerman et al., 2018; Lechtenfeld et al., 2014), this supports the dominance of modern and fresh DOC exported by the Amazon (Mayorga et al., 2005).

During low flow periods, the IOS fraction decreased, at which time more biolabile compounds from groundwater, algal inputs, and particulate organic matter (POM) have been suggested to support microbial respiration within the Amazon River (Benner et al., 1995; Vannote et al., 1980; Ward et al., 2013). Additionally, seasonal changes in Amazon River microbial communities may also have contributed to the differences in DOM biolability; particularly during the dry season where there are higher proportions of cyanobacteria in the mainstem (Doherty et al., 2017) producing more aliphatic and protein-like DOM (Bittar et al., 2015). Many of these DOM compounds are likely processed downstream of Óbidos where other clearwater tributaries including the Tapajos and Xingu Rivers join with the Amazon River before delivering DOM into the Amazon Plume and ultimately the Atlantic Ocean. For instance, although the Tapajos and Xingu Rivers only contribute less than 10% of the total Amazon River DOC flux to the Atlantic Ocean (Raymond & Spencer, 2015), they have been shown to enhance microbial degradation of terrestrial mainstem DOM through priming with biolabile compounds (Ward et al., 2016). An increase in aliphatic and protein-like DOM in the Amazon River during low discharge periods may further increase the degradation of terrestrial DOM downstream of Óbidos through priming, potentially exporting more processed DOM into the Amazon River Plume and leading to increased aquatic respiration downstream. However, the increase in biolability detected at Óbidos was likely small given the overall stable nature of Amazon DOM, which has already undergone upstream processing (Quay et al., 1992). Thus, predictable variations in seasonal hydrology offer a reasonable justification for the bulk DOM compositions at Óbidos, which have been suggested to respond

Table 1
Mean Values for FT-ICR MS-Derived DOM Compositions in the La Niña Year (August 2011–July 2012, n = 10) and the Normal Year (August 2012–July 2013, n = 12) of the Study Period ± 1σ Standard Deviation. Statistical Significance (α = 0.05) Between the Two Means was Evaluated Using a T-Test

	August 2011–July 2012 "La Niña year"	August 2012–July 2013 "normal year"	*p*
Mass (Da)	428.1332 ± 10	404.7946 ± 18	0.0014
H/C	1.09 ± 0.01	1.12 ± 0.02	0.0029
O/C	0.40 ± 0.01	0.39 ± 0.01	0.014
C_{OX}	−0.29 ± 0.03	−0.34 ± 0.04	0.0042
AI_{mod}	0.36 ± 0.01	0.35 ± 0.01	0.0029
$N_{Formula}$	7,523 ± 190	6,289 ± 1,455	0.0080
S/C (x10^3)	5.9 ± 0.5	6.5 ± 0.7	0.030
P/C (x10^3)	3.5 ± 0.9	4.6 ± 0.7	0.0039
N/C (x10^3)	30.8 ± 1.1	29.6 ± 4.0	0.33
%IOS	6.0 ± 0.01	4.8 ± 0.01	0.0018

to different discharge conditions (Seidel et al., 2016) despite extensive upstream processing of biolabile compounds within the mainstem (Hedges et al., 1994).

3.4. Changes in Amazon River DOM Composition During La Niña

While several studies have identified seasonal variations in Amazon River DOM, the absence of long-term DOC concentration and DOM composition data has made it difficult to characterize interannual patterns in Amazon River export. For instance, during the 2011–2012 La Niña, differences in Amazon River discharge were observed and attributed to the ENSO event, but not DOM composition (Medeiros et al., 2015; Seidel et al., 2016). In this study, high frequency sampling revealed that the difference in discharge between the years (271 km^3 yr^{-1}) was also accompanied by shifts in the DOM molecular properties at Óbidos. In the La Niña year, DOM was significantly ($p < 0.05$) larger, more aromatic, oxygenated, and had less *S* and *P*-containing compounds than in the normal year (Figure 4, Table 1). Additionally, the average proportion of IOS compounds was significantly higher in the La Niña year (6.0%) than in the normal year (4.8%, $p = 0.0018$), but average N/C ratios remained unchanged (Figure 4, Table 1). The La Niña year samples also contained more overall molecular formulae than in the normal year wet and dry seasons (Table 1; Table S1), suggesting that the increased precipitation from the La Niña event mobilized DOM from more diverse terrestrial sources into the Amazon River (Casas-Ruiz et al, 2020). The absence of these molecular formulae in the normal year samples, particularly in the dry season (Table S1), suggests that these compounds were not mobilized from upland sources during low discharge periods and/or that the river may contain many *in situ* microbially processed DOM compounds in the dry season that were not ionized efficiently during analysis. This is likely because negative electrospray FT-ICR MS is highly selective to aromatic carboxylic acids which are prevalent in soils and plant material and are often preferentially ionized over more aliphatic and microbial DOM that often contain basic functional groups (Sleighter & Hatcher, 2007). These changes suggest that the La Niña event mobilized DOM of more terrestrial character into the Amazon River, and subsequently exported to the Atlantic Ocean, than during the normal year.

While molecular-level aromaticity within the Amazon River has been suggested to follow seasonal variations in discharge (Seidel et al., 2016), we further demonstrate that terrestrial DOM within the Amazon River is: (1) greater at peak discharge during a La Niña year than at peak discharge during the normal year; and (2) greater across both the wet and dry seasons of a La Niña year than during peak discharge of the normal year (Figure 4). This suggests that ENSO events have the potential to influence the DOM composition exported from the Amazon River over the course of an entire year, including both the wet and dry seasons. To illustrate, a Jaccard dissimilarity matrix of all the samples indicated that during the normal year, DOM from the dry and wet seasons were distinct, each clustering separately (Figure 5a) as is expected by the mobilization of heterogeneous sources (Johnston et al., 2018; Mann et al., 2014; McLaughlin & Kaplan, 2013; Spencer et al., 2008). In contrast, DOM compositions across the entire La Niña year (2011–July 2012) were homogenous and did not follow this normal year trend, instead they resembled wet season DOM from the normal year (Figure 5a). Additionally, the changes in Amazon River DOM composition during La Niña contained many compounds that were absent from the following year, as illustrated by its high dissimilarity to the group of common molecules found in all the Amazon samples (Figure 5b). Generally, this percent dissimilarity is analogous to molecular diversity, determined from molecular richness, and follows the normal year hydrograph (Figure 5b). However, it remained constant during the La Niña year (Figure 5b), potentially skipping a natural seasonal beat in Amazonian DOM export.

Although the 6-month lag period is strongly supported by the discharge, DOC flux, and inorganic ion data (Figure 2), we further investigated various lag periods on the DOM composition at Óbidos to confirm the separation between the years. Relative intensities of all molecular formulae from the Amazon River were

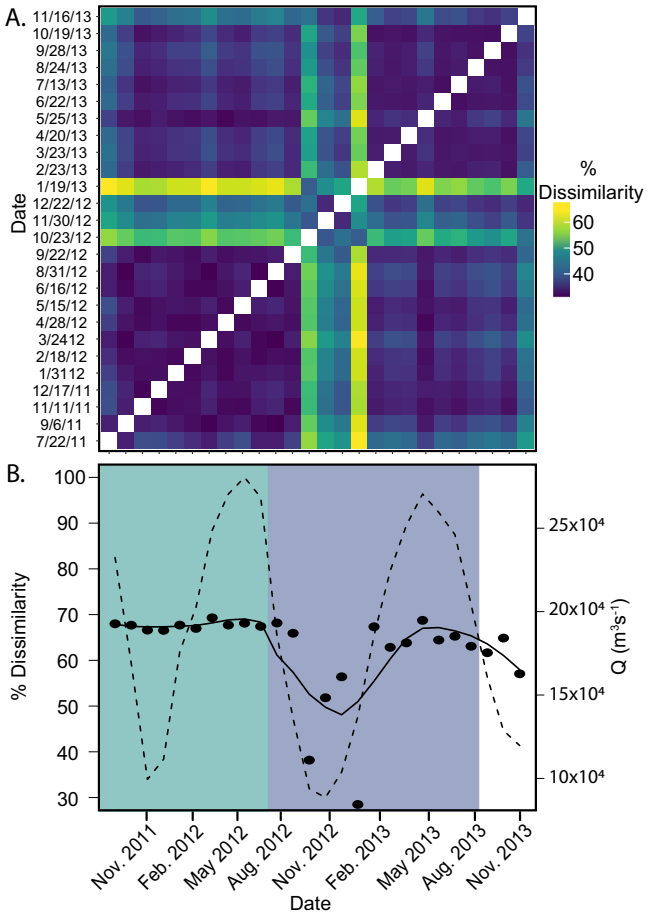

Figure 5. (a) Jaccard dissimilarity matrix of Amazon dissolved organic matter (DOM) during the study period. (b) The percent dissimilarity between each DOM sample and the group of molecules common across all Amazon samples with a fitted loess regression (solid black line). Discharge (Q) is indicated by the dashed line and study periods are divided into the La Niña year (August 2011–July 2012; green) and the normal year (August 2012–July 2013; blue).

regressed against ONI values ranging from a 0 to 12-month lag period, where a 0-month lag period was just the ONI values measured the same month that DOM was sampled, and a 12-month lag period included ONI values measured 12 months prior to DOM sampling. The number of significantly correlated ($p < 0.05$) molecular formulae was lowest at 0 months (233) and peaked (3,537) at a 6-month lag period before decreasing through 12 months (850) (Figure 6a). A similar pattern was observed by correlating formula intensities using the SOI-lagged values, which also peaked at 6 months (Figure S1a); illustrating the utility of both indices to predict changes in Amazon River DOM composition. DOM correlations with 6-month lagged ONI values followed compositional patterns driven by hydrology (Figure 6b). Compounds that correlated positively with the ONI (red points, Figure 6b) were more abundant during normal (non-ENSO) conditions and were more saturated and oxygen-deficient than La Niña DOM, suggesting greater biolability (D'Andrilli et al., 2015; Riedel et al., 2016). In contrast, formulae correlated negatively with the ONI (blue points, Figure 6b), meaning they were more abundant during La Niña, were highly aromatic and oxygenated reflecting their presumed terrestrial origins (D'Andrilli et al., 2015; Riedel et al., 2016) and suggestive of greater photolability and hydrophilicity (Riedel et al., 2016; Stubbins et al., 2010). An analogous trend was observed with 6-month lagged SOI correlations, though the correlations were inverted since La Niña events are indicated by positive SOI values (Figure S1b). Furthermore, given the bimodal nature of yearly discharge in the Amazon River (Figure 3), there was no periodicity of significantly correlated formulae with 18-month lagged ONI values (Table S2), strongly suggesting that Amazon River DOM composition is influenced by interannual ENSO cycles in addition to seasonal hydrology.

3.5. Implications of Future ENSO Events on Amazonian DOM Export and Carbon Cycling

Our data suggests that the composition of Amazon River DOM is likely dependent on how La Niña, and other ENSO events, influence each region within the basin and subsequently, the DOM exported from each tributary. For instance, heavy precipitation during the La Niña event under study here was focused mostly in the Northern and Western sub-catchments, as has typically occurred in past La Niña events (Espinoza et al., 2013; Marengo et al., 2013). The Northern regions drain into the mainstem via the blackwater Rio Negro and the western regions feed the whitewater Rio Solimões. These tributaries join upstream of Óbidos, together contributing the majority of DOC in the Amazon River (Moreira- Turcq et al, 2003). The Rio Negro exports predominantly aromatic and polyphenolic compounds into the mainstem, while whitewater tributaries adsorb this material to their sediment load upon mixing and contribute relatively more aliphatic compounds (Gonsior et al., 2016). However, different precipitation patterns could alter the proportion and composition of DOM exported from each tributary. For example, greater precipitation in the Rio Negro Basin and Northeast alone would have leached more aromatic DOM into the tributary from organic-rich soils, possibly overwhelming the adsorptive capacity of fine suspended sediment from the Solimões (Gonsior et al., 2016; Pérez et al., 2011), resulting in even more aromatic and IOS compounds exported to the mainstem. In contrast, had the La Niña caused more precipitation in the south than the north, fine suspended sediment from the Peruvian and Bolivian Andes might have adsorbed more aromatic DOM from the Rio Negro as the tributaries mixed, lowering the aromaticity and nitrogen content of the DOM in the Amazon River (Aufdenkampe et al., 2001; Aufdenkampe et al., 2007; Pérez et al., 2011). Additionally, differences in the amount of dissolved ions mobilized into the Amazon River would likely also affect the DOM composition measured at Óbidos as divalent cations such as Mg^{2+} and Ca^{2+} often coadsorb DOM to minerals, while

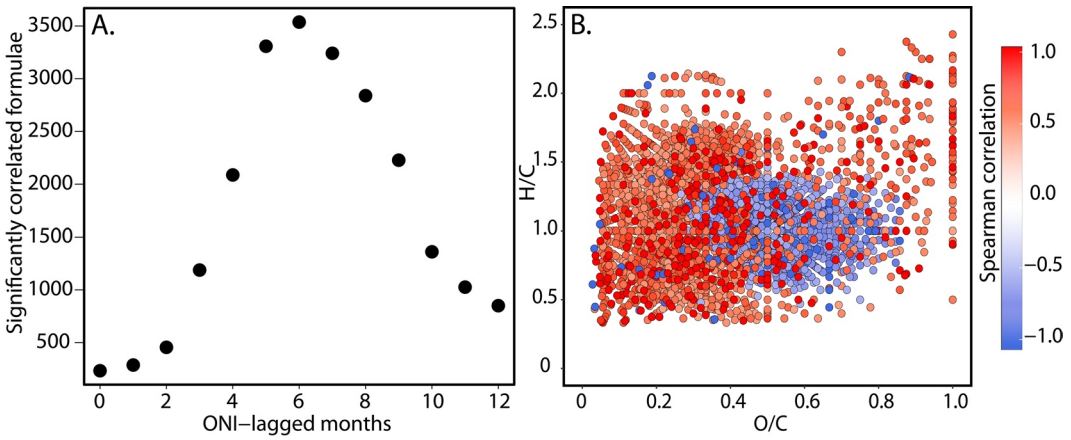

Figure 6. (a) Total number of significantly correlated molecular formulae with Oceanic Niño Index (ONI) values lagging from 0 to 12 months. (b) van Krevelen diagram of formulae correlated with ONI values from a 6-month lag period. Red points are positively correlated with ONI values while blue points are negatively correlated with ONI values.

SO_4^{2-} and PO_4^{3-} might compete with DOM functional groups for binding sites, further fractionating the DOM compositions (Groeneveld et al., 2020). POM compositions have also varied across the Amazon River continuum and may influence the DOM compositions through dissolution and degradation especially as the source material responds to changes in seasonal hydrology (Ward et al., 2013; Ward et al., 2015). Thus, the extent and location of precipitation anomalies within the Amazon Basin determine the sources and quality of DOM exported from the tributaries into the mainstem, which could subsequently impact the rate of mineralization in the Amazon and its fate downstream before it reaches the Atlantic Ocean.

The Amazon River emits vast amounts of CO_2 to the atmosphere (Richey et al., 2002; Sawakuchi et al., 2017) with annual fluxes potentially susceptible to changes in climate and land use (Aufdenkampe et al., 2011; Spencer et al., 2019). We propose that DOM compositions exported from the Amazon River will likely vary with future ENSO cycles, which are expected to increase in frequency and intensity this century from anthropogenic climate change (Cai et al., 2015; Widlansky et al., 2015). More frequent La Niña events may result in greater riverine discharge at Óbidos (Foley et al., 2002; Ronchail et al., 2005), exporting more terrestrial aromatic DOM into the Atlantic Ocean with a lower potential for microbial mineralization during transport and in the river plume. However, this might also lead to greater photooxidation of DOM, which is typically only a minor source of CO_2 in the Amazon Basin (Amon & Benner, 1996b; Remington et al., 2011), but is an important degradation process for organic-rich waters particularly in coastal ecosystems and in the Amazon Plume (Medeiros et al., 2015; Seidel et al., 2015; Stubbins et al., 2010). In contrast, more frequent El Niño events could export less DOC and terrestrial DOM into the Amazon River as a result of decreased regional rainfall and reduced hydrologic connectivity (Foley et al., 2002; Ronchail et al., 2005). Though an El Niño event was not captured during this study, we expect DOM composition in the Amazon River sampled during an El Niño year to also differ from a non-ENSO year with opposite molecular trends of what was observed during the La Niña year (Figures 4 and 5). For example, El Niño events have recently been shown to influence the amount of fluorescent DOM exported from a small subtropical watershed to the Pacific Ocean (Qu et al., 2020). Although the El Niño caused an increase in precipitation in this watershed due to geographical differences (the opposite of what occurs in the Amazon), the effects show that positive sea surface temperature anomalies in the Pacific Ocean can also influence riverine DOM export, and will likely also occur in other large watersheds, including the Amazon Basin.

Given that past ENSO-related events have been linked to predictable changes in the Amazon Basin carbon balance (Foley et al., 2002; Hastie et al., 2019), it is likely that future events may also influence both regional terrestrial and aquatic carbon cycling. Overall, we hypothesize that ENSO-related events will increase arrhythmic variations in exported DOM compositions and will impact future CO_2 fluxes from the Amazon River, possibly increasing pCO_2 from respiration of mobilized DOM compounds (D'Andrilli et al., 2019; Valle et al., 2018). In addition to the monthly sea surface temperature cycles of ENSO, other long-term

patterns such as the Pacific Decadal Oscillation and Interdecadal Pacific Oscillation may also influence Amazon River carbon cycling, as these low-frequency variations have partly been responsible for the increased seasonality in Amazon River discharge over the past 30 years (Liang et al., 2020). Though the long-term effects of ENSO, and other low-frequency sea surface temperature oscillations, on Amazonian and global carbon balance currently remains speculative, the differences in DOC fluxes and DOM composition observed between a La Niña and a normal year along with the projected increase in ENSO events suggest that discharge, DOC, DOM composition, and CO_2 fluxes must be continually assessed in long-term datasets to better understand their contributions to the global carbon cycle and their susceptibility to interannual variations in precipitation patterns. This includes considerations as to where studies will be conducted within the basin since tributaries export DOM from various sources and may not all be equally mobilized by ENSO events.

Conflict of Interest

The authors declare no conflicts of interest relevant to this study.

Data Availability Statement

The authors declare that all data supporting the results of this study are archived in the EarthChem Library (https://doi.org/10.26022/IEDA/111816) and are currently available as supplemental files.

Acknowledgments
The authors would like to thank Ina Ulber and Ekaterina Bulygina for assistance with sample processing, and a network of collaborators in Santarem, Brazil for their local expertize and logistical assistance. This work was partially supported by National Science Foundation grant OCE-1464396 to Robert G. M. Spencer and funding from the Harbourton Foundation to Robert G. M. Spencer, R. Max Holmes, and Bernhard Peucker-Ehrenbrink.

References

Amon, R. M. W., & Benner, R. (1996a). Bacterial utilization of different size classes of dissolved organic matter. *Limnology & Oceanography*, *41*(1), 41–51. https://doi.org/10.4319/lo.1996.41.1.0041

Amon, R. M. W., & Benner, R. (1996b). Photochemical and microbial consumption of dissolved organic carbon and dissolved oxygen in the Amazon River system. *Geochimica et Cosmochimica Acta*, *60*(10), 1783–1792. https://doi.org/10.1016/0016-7037(96)00055-5

Aufdenkampe, A. K., Hedges, J. I., Richey, J. E., Krusche, A. V., & Llerena, C. A. (2001). Sorptive fractionation of dissolved organic nitrogen and amino acids onto fine sediments within the Amazon Basin. *Limnology & Oceanography*, *46*(8), 1921–1935. https://doi.org/10.4319/lo.2001.46.8.1921

Aufdenkampe, A. K., Mayorga, E., Hedges, J. I., Llerena, C., Quay, P. D., Gudeman, J., et al. (2007). Organic matter in the Peruvian headwaters of the Amazon: Compositional evolution from the Andes to the lowland Amazon mainstem. *Organic Geochemistry*, *38*(3), 337–364. https://doi.org/10.1016/j.orggeochem.2006.06.003

Aufdenkampe, A. K., Mayorga, E., Raymond, P. A., Melack, J. M., Doney, S. C., Alin, S. R., et al. (2011). Riverine coupling of biogeochemical cycles between land, oceans, and atmosphere. *Frontiers in Ecology and the Environment*, *9*(1), 53–60. https://doi.org/10.1890/100014

Australian Government Bureau of Meteorology. (2020). Australian Government Bureau of Meterology Southern Oscillation Index (SOI) since 1876. Retrieved from http://www.bom.gov.au/climate/current/soihtm1.shtml

Battin, T. J., Luyssaert, S., Kaplan, L. A., Aufdenkampe, A. K., Richter, A., & Tranvik, L. J. (2009). The boundless carbon cycle. *Nature Geoscience*, *2*(9), 598–600. https://doi.org/10.1038/ngeo618

Benjamini, Y., & Hochberg, Y. (1995). Controlling the false discovery rate: A practical and powerful approach to multiple testing. *Journal of the Royal Statistical Society: Series B*, *57*(1), 289–300. https://doi.org/10.1111/j.2517-6161.1995.tb02031.x

Benner, R., Opsahl, S., Chin-Leo, G., Richey, J. E., & Forsberg, B. R. (1995). Bacterial carbon metabolism in the Amazon River system. *Limnology & Oceanography*, *40*(7), 1262–1270. https://doi.org/10.4319/lo.1995.40.7.1262

Bittar, T. B., Stubbins, A., Vieira, A. A., & Mopper, K. (2015). Characterization and photodegradation of dissolved organic matter (DOM) from a tropical lake and its dominant primary producer, the cyanobacteria Microcystis aeruginosa. *Marine Chemistry*, *177*, 205–217. https://doi.org/10.1016/j.marchem.2015.06.016

Brown, K. A., Williams, W. J., Carmack, E. C., Fiske, G., François, R., McLennan, D., & Peucker-Ehrenbrink, B. (2020). Geochemistry of small Canadian Arctic Rivers with diverse geological and hydrological settings. *Journal of Geophysical Research: Biogeosciences*, *125*(1), e2019JG005414. https://doi.org/10.1029/2019jg005414

Cai, W., Santoso, A., Wang, G., Yeh, S. W., An, S. I., Cobb, K. M., et al. (2015). ENSO and greenhouse warming. *Nature Climate Change*, *5*(9), 849–859. https://doi.org/10.1038/nclimate2743

Casas-Ruiz, J. P., Spencer, R. G., Guillemette, F., von Schiller, D., Obrador, B., Podgorski, D. C., et al. (2020). Delineating the continuum of dissolved organic matter in temperate river networks. *Global Biogeochemical Cycles*, *34*(8), e2019GB006495. https://doi.org/10.1029/2019GB006495

Cole, J. J., Prairie, Y. T., Caraco, N. F., McDowell, W. H., Tranvik, L. J., Striegl, R. G., et al. (2007). Plumbing the global carbon cycle: Integrating inland waters into the terrestrial carbon budget. *Ecosystems*, *10*(1), 172–185. https://doi.org/10.1007/s10021-006-9013-8

D'Andrilli, J., Cooper, W. T., Foreman, C. M., & Marshall, A. G. (2015). An ultrahigh-resolution mass spectrometry index to estimate natural organic matter lability. *Rapid Communications in Mass Spectrometry*, *29*(24), 2385–2401. https://doi.org/10.1002/rcm.7400

D'Andrilli, J., Junker, J. R., Smith, H. J., Scholl, E. A., & Foreman, C. M. (2019). DOM composition alters ecosystem function during microbial processing of isolated sources. *Biogeochemistry*, *142*(2), 281–298.

Devol, A. H., Forsberg, B. R., Richey, J. E., & Pimentel, T. P. (1995). Seasonal variation in chemical distributions in the Amazon (Solimoes) River: A multiyear time series. *Global Biogeochemical Cycles*, *9*(3), 307–328. https://doi.org/10.1029/95gb01145

Dittmar, T., Koch, B., Hertkorn, N., & Kattner, G. (2008). A simple and efficient method for the solid-phase extraction of dissolved organic matter (SPE-DOM) from seawater. *Limnology and Oceanography: Methods*, *6*(6), 230–235. https://doi.org/10.4319/lom.2008.6.230

Doherty, M., Yager, P. L., Moran, M. A., Coles, V. J., Fortunato, C. S., Krusche, A. V., et al. (2017). Bacterial biogeography across the Amazon River-ocean continuum. *Frontiers in Microbiology*, *8*, 882. https://doi.org/10.3389/fmicb.2017.00882

Dornblaser, M. M., & Striegl, R. G. (2009). Suspended sediment and carbonate transport in the Yukon River Basin, Alaska: Fluxes and potential future responses to climate change. *Water Resources Research*, *45*(6). https://doi.org/10.1029/2008wr007546

Drake, T. W., Hemingway, J. D., Kurek, M. R., Peucker-Ehrenbrink, B., Brown, K. A., Holmes, R. M., et al. (2021). The Pulse of the Amazon: Fluxes of dissolved organic carbon, nutrients, and ions from the world's largest river. *Global Biogeochemical Cycles*, *35*, e2020GB006895. https://doi.org/10.1029/2020GB006895

Drake, T. W., Raymond, P. A., & Spencer, R. G. (2018). Terrestrial carbon inputs to inland waters: A current synthesis of estimates and uncertainty. *Limnology and Oceanography Letters*, *3*(3), 132–142. https://doi.org/10.1002/lol2.10055

Ertel, J. R., Hedges, J. I., Devol, A. H., Richey, J. E., & Ribeiro, M. D. N. G. (1986). Dissolved humic substances of the Amazon River system 1. *Limnology & Oceanography*, *31*(4), 739–754. https://doi.org/10.4319/lo.1986.31.4.0739

Espinoza, J. C., Marengo, J. A., Ronchail, J., Carpio, J. M., Flores, L. N., & Guyot, J. L. (2014). The extreme 2014 flood in south-western Amazon basin: The role of tropical-subtropical South Atlantic SST gradient. *Environmental Research Letters*, *9*(12), 124007. https://doi.org/10.1088/1748-9326/9/12/124007

Espinoza, J. C., Ronchail, J., Frappart, F., Lavado, W., Santini, W., & Guyot, J. L. (2013). The major floods in the Amazonas River and tributaries (Western Amazon basin) during the 1970–2012 period: A focus on the 2012 flood. *Journal of Hydrometeorology*, *14*(3), 1000–1008. https://doi.org/10.1175/jhm-d-12-0100.1

Foley, J. A., Botta, A., Coe, M. T., & Costa, M. H. (2002). El Niño–Southern oscillation and the climate, ecosystems and rivers of Amazonia. *Global Biogeochemical Cycles*, *16*(4), 1132. https://doi.org/10.1029/2002gb001872

Gonsior, M., Valle, J., Schmitt-Kopplin, P., Hertkorn, N., Bastviken, D., Luek, J., et al. (2016). Chemodiversity of dissolved organic matter in the Amazon Basin. *Biogeosciences*, *13*(14), 4279–4290. https://doi.org/10.5194/bg-13-4279-2016

Groeneveld, M., Catalán, N., Attermeyer, K., Hawkes, J., Einarsdóttir, K., Kothawala, D., et al. (2020). Selective adsorption of terrestrial dissolved organic matter to inorganic surfaces along a boreal inland water continuum. *Journal of Geophysical Research: Biogeosciences*, *125*(3), e2019JG005236. https://doi.org/10.1029/2019jg005236

Hastie, A., Lauerwald, R., Ciais, P., & Regnier, P. (2019). Aquatic carbon fluxes dampen the overall variation of net ecosystem productivity in the Amazon basin: An analysis of the interannual variability in the boundless carbon cycle. *Global Change Biology*, *25*(6), 2094–2111. https://doi.org/10.1111/gcb.14620

Hedges, J. I., Clark, W. A., Quay, P. D., Richey, J. E., Devol, A. H., & Santos, M. (1986). Compositions and fluxes of particulate organic material in the Amazon River 1. *Limnology & Oceanography*, *31*(4), 717–738. https://doi.org/10.4319/lo.1986.31.4.0717

Hedges, J. I., Cowie, G. L., Richey, J. E., Quay, P. D., Benner, R., Strom, M., & Forsberg, B. R. (1994). Origins and processing of organic matter in the Amazon River as indicated by carbohydrates and amino acids. *Limnology & Oceanography*, *39*(4), 743–761. https://doi.org/10.4319/lo.1994.39.4.0743

Hedges, J. I., Keil, R. G., & Benner, R. (1997). What happens to terrestrial organic matter in the ocean? *Organic Geochemistry*, *27*(5–6), 195–212. https://doi.org/10.1016/s0146-6380(97)00066-1

Johnston, S. E., Shorina, N., Bulygina, E., Vorobjeva, T., Chupakova, A., Klimov, S. I., et al. (2018). Flux and seasonality of dissolved organic matter from the Northern Dvina (Severnaya Dvina) River, Russia. *Journal of Geophysical Research: Biogeosciences*, *123*(3), 1041–1056. https://doi.org/10.1002/2017jg004337

Kellerman, A. M., Guillemette, F., Podgorski, D. C., Aiken, G. R., Butler, K. D., & Spencer, R. G. (2018). Unifying concepts linking dissolved organic matter composition to persistence in aquatic ecosystems. *Environmental Science & Technology*, *52*(5), 2538–2548. https://doi.org/10.1021/acs.est.7b05513

Koch, B. P., & Dittmar, T. (2006). From mass to structure: An aromaticity index for high-resolution mass data of natural organic matter. *Rapid Communications in Mass Spectrometry*, *20*(5), 926–932. https://doi.org/10.1002/rcm.2386

Koch, B. P., & Dittmar, T. (2016). From mass to structure: An aromaticity index for high-resolution mass data of natural organic matter. *Rapid Communications in Mass Spectrometry*, *30*, 250. https://doi.org/10.1002/rcm.7433

Kurek, M. R., Poulin, B. A., McKenna, A. M., & Spencer, R. G. (2020). Deciphering dissolved organic matter: Ionization, dopant, and fragmentation insights via fourier transform-ion cyclotron resonance mass spectrometry. *Environmental Science & Technology*, *54*(24), 16249–16259. https://doi.org/10.1021/acs.est.0c05206

Lechtenfeld, O. J., Kattner, G., Flerus, R., McCallister, S. L., Schmitt-Kopplin, P., & Koch, B. P. (2014). Molecular transformation and degradation of refractory dissolved organic matter in the Atlantic and Southern Ocean. *Geochimica et Cosmochimica Acta*, *126*, 321–337. https://doi.org/10.1016/j.gca.2013.11.009

Liang, Y. C., Lo, M. H., Lan, C. W., Seo, H., Ummenhofer, C. C., Yeager, S., et al. (2020). Amplified seasonal cycle in hydroclimate over the Amazon River basin and its plume region. *Nature Communications*, *11*(1), 1–11. https://doi.org/10.1038/s41467-020-18187-0

Mann, B. F., Chen, H., Herndon, E. M., Chu, R. K., Tolic, N., Portier, E. F., et al. (2015). Indexing permafrost soil organic matter degradation using high-resolution mass spectrometry. *PLoS One*, *10*(6), e0130557. https://doi.org/10.1371/journal.pone.0130557

Mann, P. J., Davydova, A., Zimov, N., Spencer, R. G. M., Davydov, S., Bulygina, E., et al. (2012). Controls on the composition and lability of dissolved organic matter in Siberia's Kolyma River basin. *Journal of Geophysical Research*, *117*(G1). G01028. https://doi.org/10.1029/2011jg001798

Mann, P. J., Spencer, R. G. M., Dinga, B. J., Poulsen, J. R., Hernes, P. J., Fiske, G., et al. (2014). The biogeochemistry of carbon across a gradient of streams and rivers within the Congo Basin. *Journal of Geophysical Research: Biogeosciences*, *119*(4), 687–702. https://doi.org/10.1002/2013jg002442

Marengo, J. A., Alves, L. M., Soares, W. R., Rodriguez, D. A., Camargo, H., Riveros, M. P., & Pabló, A. D. (2013). Two contrasting severe seasonal extremes in tropical South America in 2012: Flood in Amazonia and drought in northeast Brazil. *Journal of Climate*, *26*(22), 9137–9154. https://doi.org/10.1175/jcli-d-12-00642.1

Mayorga, E., Aufdenkampe, A. K., Masiello, C. A., Krusche, A. V., Hedges, J. I., Quay, P. D., et al. (2005). Young organic matter as a source of carbon dioxide outgassing from Amazonian rivers. *Nature*, *436*(7050), 538–541. https://doi.org/10.1038/nature03880

McLaughlin, C., & Kaplan, L. A. (2013). Biological lability of dissolved organic carbon in stream water and contributing terrestrial sources. *Freshwater Science*, *32*(4), 1219–1230. https://doi.org/10.1899/12-202.1

Medeiros, P. M., Seidel, M., Ward, N. D., Carpenter, E. J., Gomes, H. R., Niggemann, J., et al. (2015). Fate of the Amazon River dissolved organic matter in the tropical Atlantic Ocean. *Global Biogeochemical Cycles*, *29*(5), 677–690. https://doi.org/10.1002/2015gb005115

Moquet, J. S., Guyot, J. L., Crave, A., Viers, J., Filizola, N., Martinez, J. M., et al. (2016). Amazon River dissolved load: Temporal dynamics and annual budget from the Andes to the ocean. *Environmental Science and Pollution Research*, *23*(12), 11405–11429. https://doi.org/10.1007/s11356-015-5503-6

Moreira-Turcq, P., Seyler, P., Guyot, J. L., & Etcheber, H. (2003). Exportation of organic carbon from the Amazon River and its main tributaries. *Hydrological Processes*, *17*(7), 1329–1344.

National Weather Service Climate Predicition Center. (2020). Cold & warm episodes by season. https://origin.cpc.ncep.noaa.gov/products/analysis_monitoring/ensostuff/ONI_v5.php

Pang, Y., Wang, K., Sun, Y., Zhou, Y., Yang, S., Li, Y., et al. (2021). Linking the unique molecular complexity of dissolved organic matter to flood period in the Yangtze River mainstream. *The Science of the Total Environment*, *764*, 142803. https://doi.org/10.1016/j.scitotenv.2020.142803

Pérez, M. A., Moreira-Turcq, P., Gallard, H., Allard, T., & Benedetti, M. F. (2011). Dissolved organic matter dynamic in the Amazon basin: Sorption by mineral surfaces. *Chemical Geology*, *286*(3–4), 158–168. https://doi.org/10.1016/j.chemgeo.2011.05.004

Qu, L., Wu, Y., Li, Y., Stubbins, A., Dahlgren, R. A., Chen, N., & Guo, W. (2020). El Niño-Driven dry season flushing enhances dissolved organic matter export from a subtropical watershed. *Geophysical Research Letters*, *47*(19), e2020GL089877. https://doi.org/10.1029/2020gl089877

Quay, P. D., Wilbur, D. 0., Richey, J. E., Hedges, J. I., Devol, A. H., & Victoria, R. (1992). Carbon cycling in the Amazon River: Implications from the 13C compositions of particles and solutes. *Limnology & Oceanography*, *37*(4), 857–871. https://doi.org/10.4319/lo.1992.37.4.0857

Raymond, P. A., & Spencer, R. G. (2015). Riverine DOM. In *Biogeochemistry of marine dissolved organic matter*. Academic Press. (pp. 509–533). https://doi.org/10.1016/b978-0-12-405940-5.00011-x

Remington, S., Krusche, A., & Richey, J. (2011). Effects of DOM photochemistry on bacterial metabolism and CO_2 evasion during falling water in a humic and a whitewater river in the Brazilian Amazon. *Biogeochemistry*, *105*(1–3), 185–200. https://doi.org/10.1007/s10533-010-9565-8

Revelle, W. R. (2017). psych: Procedures for personality and psychological research.

Richey, J. E., Hedges, J. I., Devol, A. H., Quay, P. D., Victoria, R., Martinelli, L., & Forsberg, B. R. (1990). Biogeochemistry of carbon in the Amazon River. *Limnology & Oceanography*, *35*(2), 352–371. https://doi.org/10.4319/lo.1990.35.2.0352

Richey, J. E., Melack, J. M., Aufdenkampe, A. K., Ballester, V. M., & Hess, L. L. (2002). Outgassing from Amazonian rivers and wetlands as a large tropical source of atmospheric CO_2. *Nature*, *416*(6881), 617–620. https://doi.org/10.1038/416617a

Richey, J. E., Nobre, C., & Deser, C. (1989). Amazon River discharge and climate variability: 1903 to 1985. *Science*, *246*(4926), 101–103. https://doi.org/10.1126/science.246.4926.101

Riedel, T., & Dittmar, T. (2014). A method detection limit for the analysis of natural organic matter via Fourier transform ion cyclotron resonance mass spectrometry. *Analytical Chemistry*, *86*(16), 8376–8382. https://doi.org/10.1021/ac501946m

Riedel, T., Zark, M., Vähätalo, A. V., Niggemann, J., Spencer, R. G., Hernes, P. J., & Dittmar, T. (2016). Molecular signatures of biogeochemical transformations in dissolved organic matter from ten world rivers. *Frontiers of Earth Science*, *4*, 85. https://doi.org/10.3389/feart.2016.00085

Ronchail, J., Labat, D., Callede, J., Cochonneau, G., Guyot, J. L., Filizola, N., & De Oliveira, E. (2005). Discharge variability within the Amazon basin. In *Regional hydrological impacts of climatic change: Hydroclimatic variability: Proceedings of symposium S6 held during the seventh IAHS scientific assembly* (pp. 21–9). International Association of Hydrological Sciences.

Rose, L. A., Karwan, D. L., & Godsey, S. E. (2018). Concentration–discharge relationships describe solute and sediment mobilization, reaction, and transport at event and longer timescales. *Hydrological Processes*, *32*(18), 2829–2844. https://doi.org/10.1002/hyp.13235

Runkel, R. L., Crawford, C. G., & Cohn, T. A. (2004). *Load estimator (LOADEST): A FORTRAN program for estimating constituent loads in streams and rivers (No. 4–A5)*.

Sawakuchi, H. O., Neu, V., Ward, N. D., Barros, M. D. L. C., Valerio, A. M., Gagne-Maynard, W., et al. (2017). Carbon dioxide emissions along the lower Amazon River. *Frontiers in Marine Science*, *4*, 76. https://doi.org/10.3389/fmars.2017.00076

Seidel, M., Dittmar, T., Ward, N. D., Krusche, A. V., Richey, J. E., Yager, P. L., & Medeiros, P. M. (2016). Seasonal and spatial variability of dissolved organic matter composition in the lower Amazon River. *Biogeochemistry*, *131*(3), 281–302. https://doi.org/10.1007/s10533-016-0279-4

Seidel, M., Yager, P. L., Ward, N. D., Carpenter, E. J., Gomes, H. R., Krusche, A. V., et al. (2015). Molecular-level changes of dissolved organic matter along the Amazon River-to-ocean continuum. *Marine Chemistry*, *177*, 218–231. https://doi.org/10.1016/j.marchem.2015.06.019

Sleighter, R. L., & Hatcher, P. G. (2007). The application of electrospray ionization coupled to ultrahigh resolution mass spectrometry for the molecular characterization of natural organic matter. *Journal of Mass Spectrometry*, *42*(5), 559–574. https://doi.org/10.1002/jms.1221

Spencer, R. G., Aiken, G. R., Dornblaser, M. M., Butler, K. D., Holmes, R. M., Fiske, G., et al. (2013). Chromophoric dissolved organic matter export from US Rivers. *Geophysical Research Letters*, *40*(8), 1575–1579. https://doi.org/10.1002/grl.50357

Spencer, R. G., Aiken, G. R., Wickland, K. P., Striegl, R. G., & Hernes, P. J. (2008). Seasonal and spatial variability in dissolved organic matter quantity and composition from the Yukon River basin, Alaska. *Global Biogeochemical Cycles*, *22*(4). https://doi.org/10.1029/2008gb003231

Spencer, R. G., Hernes, P. J., Dinga, B., Wabakanghanzi, J. N., Drake, T. W., & Six, J. (2016). Origins, seasonality, and fluxes of organic matter in the Congo River. *Global Biogeochemical Cycles*, *30*(7), 1105–1121. https://doi.org/10.1002/2016gb005427

Spencer, R. G., Kellerman, A. M., Podgorski, D. C., Macedo, M. N., Jankowski, K., Nunes, D., & Neill, C. (2019). Identifying the molecular signatures of agricultural expansion in Amazonian headwater streams. *Journal of Geophysical Research: Biogeosciences*, *124*(6), 1637–1650. https://doi.org/10.1029/2018jg004910

Stedmon, C. A., Amon, R. M. W., Rinehart, A. J., & Walker, S. A. (2011). The supply and characteristics of colored dissolved organic matter (CDOM) in the Arctic Ocean: Pan Arctic trends and differences. *Marine Chemistry*, *124*(1–4), 108–118. https://doi.org/10.1016/j.marchem.2010.12.007

Stubbins, A., Spencer, R. G., Chen, H., Hatcher, P. G., Mopper, K., Hernes, P. J., et al. (2010). Illuminated darkness: Molecular signatures of Congo River dissolved organic matter and its photochemical alteration as revealed by ultrahigh precision mass spectrometry. *Limnology & Oceanography*, *55*(4), 1467–1477. https://doi.org/10.4319/lo.2010.55.4.1467

Textor, S., Wickland, K., Podgorski, D., Johnston, S. E., & Spencer, R. G. M. (2019). Dissolved organic carbon turnover in permafrost-influenced watersheds of interior Alaska: Molecular insights and the priming effect. *Frontiers of Earth Science*, *7*, 275. https://doi.org/10.3389/feart.2019.00275

Tranvik, L. J., Downing, J. A., Cotner, J. B., Loiselle, S. A., Striegl, R. G., Ballatore, T. J., et al. (2009). Lakes and reservoirs as regulators of carbon cycling and climate. *Limnology & Oceanography*, *54*(6), 2298–2314. https://doi.org/10.4319/lo.2009.54.6_part_2.2298

Valle, J., Gonsior, M., Harir, M., Enrich-Prast, A., Schmitt-Kopplin, P., Bastviken, D., et al. (2018). Extensive processing of sediment pore water dissolved organic matter during anoxic incubation as observed by high-field mass spectrometry (FTICR-MS). *Water Research*, *129*, 252–263. https://doi.org/10.1016/j.watres.2017.11.015

Vannote, R. L., Minshall, G. W., Cummins, K. W., Sedell, J. R., & Cushing, C. E. (1980). The river continuum concept. *Canadian Journal of Fisheries and Aquatic Sciences*, *37*(1), 130–137. https://doi.org/10.1139/f80-017

Voss, B. M., Peucker-Ehrenbrink, B., Eglinton, T. I., Fiske, G., Wang, Z. A., Hoering, K. A., et al. (2014). Tracing river chemistry in space and time: Dissolved inorganic constituents of the Fraser River, Canada. *Geochimica et Cosmochimica Acta*, *124*, 283–308. https://doi.org/10.1016/j.gca.2013.09.006

Wagner, S., Fair, J. H., Matt, S., Hosen, J. D., Raymond, P., Saiers, J., et al. (2019). Molecular hysteresis: Hydrologically driven changes in riverine dissolved organic matter chemistry during a storm event. *Journal of Geophysical Research: Biogeosciences*, *124*(4), 759–774. https://doi.org/10.1029/2018jg004817

Ward, N. D., Bianchi, T. S., Sawakuchi, H. O., Gagne-Maynard, W., Cunha, A. C., Brito, D. C., et al. (2016). The reactivity of plant-derived organic matter and the potential importance of priming effects along the lower Amazon River. *Journal of Geophysical Research: Biogeosciences*, *121*(6), 1522–1539. https://doi.org/10.1002/2016jg003342

Ward, N. D., Keil, R. G., Medeiros, P. M., Brito, D. C., Cunha, A. C., Dittmar, T., et al. (2013). Degradation of terrestrially derived macromolecules in the Amazon River. *Nature Geoscience*, *6*(7), 530–533. https://doi.org/10.1038/ngeo1817

Ward, N. D., Krusche, A. V., Sawakuchi, H. O., Brito, D. C., Cunha, A. C., Moura, J. M. S., et al. (2015). The compositional evolution of dissolved and particulate organic matter along the lower Amazon River—Óbidos to the ocean. *Marine Chemistry*, *177*, 244–256. https://doi.org/10.1016/j.marchem.2015.06.013

Wickham, H. (2016). *Ggplot2: Elegant graphics for data analysis*. Springer.

Widlansky, M. J., Timmermann, A., & Cai, W. (2015). Future extreme sea level seesaws in the tropical Pacific. *Science Advances*, *1*(8), e1500560. https://doi.org/10.1126/sciadv.1500560